Damping in a Parametrically Excited Cracked Rotor

Jerzy T. Sawicki and Zbigniew Kulesza

Abstract Conducted analyses of rotors with cracked shafts show that the stability of such systems deteriorates with an increasing crack depth. Instability areas near parametric resonances enhance as a result of increasing periodic stiffness changes due to a breathing mechanism of a developing shaft crack. However, some recent studies on the dynamics of linear structures with periodically altered stiffness present an interesting phenomenon of an increase in damping. It has been demonstrated that under certain conditions a parametrically excited mechanical structure can increase its stability. When the structure falls into the parametric anti-resonant area, its vibration amplitudes quickly decay. For a long time these anti-resonant zones seemed to be not interesting, yet they can introduce additional artificial damping into the system, improving its stability and leading to further studies of their possible applications. The present paper analyzes the possibility of the appearance of such a phenomenon (the increase in damping of the parametrically excited system) in a rotor with a cracked shaft. The approach is demonstrated with a mathematical model of the machine. The breathing crack is modeled using the rigid finite element method that has previously proven its robustness and efficiency in similar applications. The stability analysis is conducted numerically by the Floquet's technique. The conditions required for the appearance of parametric anti-resonances for different crack depths are provided. Finally, a possible application of the additional damping introduced by parametric excitation for rotor crack detection is analyzed.

Keywords Cracked rotors · Parametric excitation · Stability analysis

J.T. Sawicki (✉)
Department of Mechanical Engineering, Center for Rotating Machinery Dynamics and Control, Cleveland State University, Cleveland, OH 44115-2214, USA
e-mail: j.sawicki@csuohio.edu

Z. Kulesza
Bialystok University of Technology, Faculty of Mechanical Engineering, Bialystok, Poland
e-mail: z.kulesza@pb.edu.pl

P. Pennacchi (ed.), *Proceedings of the 9th IFToMM International Conference on Rotor Dynamics*, Mechanisms and Machine Science 21,
DOI 10.1007/978-3-319-06590-8_26

1 Introduction

Parametrically excited vibrations can be explained by periodical variation of one or more coefficients of the differential equation of motion. If at least one system parameter is varied close to a *parametric excitation frequency* η_n then a parametric resonance may appear. The parametric excitation frequency is defined as follows [2–7]

$$\eta_n = \frac{|\Omega_k \mp \Omega_l|}{n}, \quad k, l = 1, 2, \ldots \tag{1}$$

where Ω_k and Ω_l are the kth and lth natural frequency of the undamped system with constant coefficients, and n is the order of the parametric resonance. For $k = l$ frequency η_n is called a *principal parametric resonance*, and for $k \neq l$—it is a *parametric combination resonance*. Usually, only first order resonances for $n = 1$ are considered.

It has been shown [2, 17] that, principal parametric resonances (for $k = l$ and the plus "+" sign in Eq. (1)) and parametric combination resonances of the summation-type (for $k \neq l$ and the plus "+" sign) always destabilize the system. However, difference-type combination resonances (for $k \neq l$ and the minus "–" sign) for parametric excitations leading to symmetric system matrices have a unique property to suppress vibrations. The specific difference-type combination excitations that stabilize an otherwise unstable system are called *parametric anti-resonances*.

Tondl was the first who demonstrated [17] that an unstable self-excited system can be stabilized by introducing periodic stiffness changes at a specific parametric anti-resonance frequency. Since then, parametric anti-resonances have been observed and studied only in combination with self-excitation. However, the pioneering works of Dohnal [2–4] showed that the properly chosen parametric anti-resonance not only stabilizes an already unstable system, but it can also increase the existing damping in a stable system. Thus, the phenomenon known as the *damping by parametric excitation* has been identified and explained as the coupling of eigenvalues of the underlying system. This stabilizing effect may be interesting for its probable ability to indicate a shaft crack.

The shaft crack, if occurs, is one of the most dangerous malfunctions of rotating machines [8, 9, 12–16]. Resulting from cyclic loading, thermal stresses, creep, corrosion and/or other mechanisms to which rotating shafts are subjected to, the transverse crack can propagate quickly to the relevant depth at which a sudden destruction of the shaft occurs. This usually leads to a catastrophic failure of the machine and that is why an early detection of shaft cracks is so important.

Shaft cracks are usually modeled with local periodic stiffness changes resulting from the *breathing mechanism*, i.e. from the constant opening and closing of the crack faces during the rotation [1, 12, 13, 15]. These stiffness changes transform the linear time-invariant rotor-bearing system into the parametrically excited one, described by linear motion equations with time-variant coefficients. This way, the

possible appearance and applications of the effect of damping by parametric excitation in rotor systems with cracked shafts can be identified and analyzed.

Similar problems have already been studied for different rotors excited parametrically. Ecker [5–7] presented numerical results for a Jeffcott rotor with time-varying stiffness and demonstrated the increase in damping as a result of axial excitations at the first anti-resonant frequency. In [5] the author obtained similar results for a rotor with periodically varied radial stiffness applied in different locations along the shaft axis. Dohnal [3, 4] conducted numerical and experimental studies of a flexible rotor supported by active magnetic bearings (AMBs) confirming the increase in damping by stiffness changes in the bearings.

Numerical stability analyzes of cracked rotors based on the Floquet's theory and focusing on parametric resonances are presented in several papers, including the most recent by Ricci and Pennacchi [14], Guo et al. [8] and Han and Chu [9].

The present paper analyzes possibility of the appearance of the damping by parametric excitation in a rotor with a cracked shaft. The approach is demonstrated with a mathematical model of the cracked rotor. The breathing crack is modeled using the rigid finite element method and the stability analysis is conducted numerically by the Floquet's technique. The conditions required for the appearance of parametric anti-resonances for different crack depths are provided. Finally, a possible application of the additional damping introduced by parametric excitation for rotor crack detection is analyzed.

2 Rotor Model

The rotor shown in Fig. 1a is a part of an experimental test rig utilized at Bialystok University of Technology. A slender, flexible rotor shaft is driven by a variable-speed motor. Two rigid disks are attached to the shaft, supported by two radial ball bearings. Main dimensions and the schematic diagram of the rotor are presented in Fig. 1b.

The mathematical model of the rotor is formulated using the rigid finite element method [11, 12]. The rotor is divided into 31 undeformable bodies called rigid finite elements (RFEs) connected with 30 massless spring-damping elements (SDEs). Global and local coordinate systems of RFEs and SDEs are shown in Fig. 1c. The bearings are modeled using two additional SDEs connecting the basis (numbered as 0) with the 3rd and 28th RFEs. For the present study the RFEs with only 4° of freedom are used (two displacements and two rotations along/about $x_{r,2}$, $x_{r,3}$ axes).

Applying the Lagrange approach, the equations of motion take the following form

$$\mathbf{M}\,\ddot{\mathbf{q}} + (\mathbf{D}_{\mathrm{d}} + \Omega\mathbf{D}_{\mathrm{G}})\dot{\mathbf{q}} + \mathbf{K}[\mathbf{q}(t)]\mathbf{q} = \mathbf{p}_{\mathrm{u}} + \mathbf{w} \tag{2}$$

where $\mathbf{M}$, $\mathbf{D}_{\mathrm{d}}$, $\mathbf{D}_{\mathrm{G}}$ and $\mathbf{K}$ are $m \times m$ mass, damping, gyroscopic and stiffness matrices, respectively; $\mathbf{p}_{\mathrm{u}}$, $\mathbf{w}$ are $m \times 1$ vectors of unbalance and gravity forces; $\mathbf{q}$ is

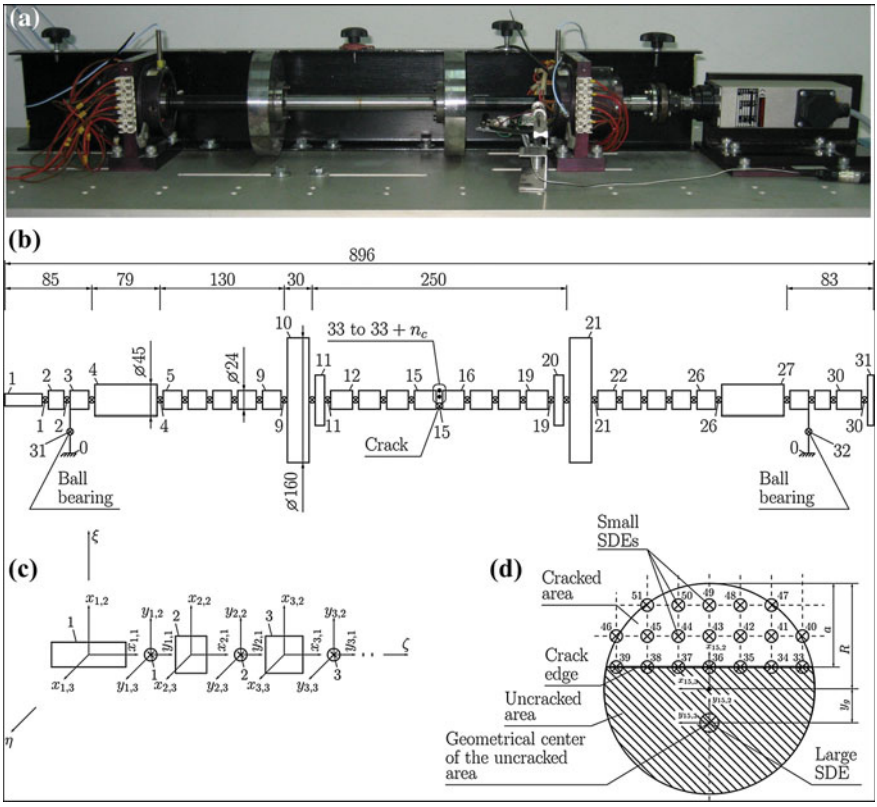

Fig. 1 Tested rotor: **a** photo, **b** RFE model, **c** coordinate systems: global ξ, η, ζ and local $x_{r,1}$, $x_{r,2}$, $x_{r,3}$ (for RFEs), $y_{k,1}$, $y_{k,2}$, $y_{k,3}$ (for SDEs), **d** shaft cross-section at the crack location

a $m \times 1$ vector of generalized coordinates of the mass centers of subsequent RFEs; Ω is rotor spin speed, $m = 4n_\mathrm{r}$, and $n_\mathrm{r} = 31$ is the number of RFEs. The stiffness matrix $\mathbf{K}$ depends on vector $\mathbf{q}$, which is in turn time-dependant. This is due to the varying stiffness of the shaft resulting from the breathing mechanism of the crack. Matrices $\mathbf{M}$, $\mathbf{D}_\mathrm{G}$ and $\mathbf{K}$ are assembled using blocks of mass $\mathbf{K}_r$, gyroscopic $\mathbf{D}_{\mathrm{G},r}$ and stiffness $\mathbf{K}_k$ coefficients defined in [11, 12]. The damping matrix $\mathbf{D}_\mathrm{d}$ is calculated from the Rayleigh's formula, as $\mathbf{D}_\mathrm{d} = \alpha_\mathrm{d}\mathbf{M} + \beta_\mathrm{d}\mathbf{K}$.

The crack is located between the 15th and 16th RFEs and is modeled using several SDEs connecting these RFEs. Figure 1d shows the cross-section of the shaft at the crack location. The relative depth μ of the crack is defined as $\mu = a/2R$, where a is the location of the crack edge line, and R is the radius of the shaft cross-section. The large SDE numbered as 15 is pinned at the geometrical center of the uncracked area and it simulates the stiffness of the uncracked portion of the shaft

cross-section. The block of stiffness coefficients $\mathbf{K}_{15}$ for this SDE is constant and proportional to the relative crack depth μ

$$\mathbf{K}_{15} = (1-\mu)\mathbf{K}_{15,\mathrm{u}} \tag{3}$$

where $\mathbf{K}_{15,\mathrm{u}}$ is the block of stiffness coefficients of the SDE, which connects the two RFEs in case of the uncracked shaft. The small SDEs simulate the stiffness of the cracked portion of the shaft cross-section. The sum of their stiffness coefficient blocks $\mathbf{K}_k$ is expressed as

$$\sum_{k=33}^{33+n_\mathrm{c}} \mathbf{K}_k = \mu\mathbf{K}_{15,\mathrm{u}} \tag{4}$$

where n_c is the number of small SDEs. During crack breathing stiffnesses of individual small SDEs are varied based on their deformations $\Delta w_{k,1}$. For the fully open crack stiffness blocks of all small SDEs are assumed as zero ($\mathbf{K}_k = \mathbf{0}$). For the fully closed crack stiffness blocks are nonzero ($\mathbf{K}_k \neq \mathbf{0}$).

3 Numerical Stability Analysis

For numerical stability analysis Eq. (2) is modified to the following form

$$\mathbf{M}\ddot{\mathbf{q}} + \mathbf{D}_\mathrm{d}\dot{\mathbf{q}} + [\mathbf{K}_0 + \mathbf{K}_\mathrm{c}\cos(\eta t)]\mathbf{q} = \mathbf{0} \tag{5}$$

where

$$\mathbf{K}_0 = \mathbf{K} - \mathbf{K}_\mathrm{c}, \mathbf{K}_c = \frac{\Delta\mathbf{K}}{2}, \Delta\mathbf{K} = \mathbf{K} - \mathbf{K}_1 \tag{6}$$

and $\mathbf{K}$, $\mathbf{K}_1$ are stiffness matrices of the healthy rotor, and the rotor with the fully open crack, respectively. Equation (5) describes the linear system, with time-variant coefficient matrix $\mathbf{K}_c \cos\eta\tau$, where η is the frequency of parametric excitation. In this numerical study the gyroscopic matrix $\mathbf{D}_\mathrm{G}$ has been neglected to better demonstrate the influence of the damping by parametric excitation effect. Thus, the rotor is not rotating and the stiffness changes due to the crack are not driven by its rotational motion but by some external loading applied to the shaft.

In order to apply the Floquet's theory Eq. (5) is transformed to the following form [2, 6, 7, 10]

$$\dot{\mathbf{x}} = \mathbf{A}(t)\mathbf{x} \tag{7}$$

with the $2m \times 1$ state vector $\mathbf{x}$ and the $2m \times 2m$ periodic matrix $\mathbf{A}(t)$ with period $T = 2\pi/\eta$, where

$$\mathbf{A}(t) = \begin{bmatrix} \mathbf{0} & \mathbf{I} \\ (-\mathbf{M}^{-1}\mathbf{K}_0 - \mathbf{M}^{-1}\mathbf{K}_c \cos \eta t) & -\mathbf{M}^{-1}\mathbf{D}_\mathrm{d} \end{bmatrix} \tag{8}$$

The stability of the periodic system given by Eq. (7) can be determined from the eigenvalues of the *monodromy matrix* $\mathbf{\Phi}(T,0)$ [2, 6, 10]

$$\mathbf{\Phi}(T,0) = [\,\mathbf{x}_1(T) \quad \mathbf{x}_2(T) \quad \ldots \quad \mathbf{x}_{2m}(T)\,] \tag{9}$$

where $\mathbf{x}_1(T), \mathbf{x}_2(T), \ldots, \mathbf{x}_{2m}(T)$ is a set of 2 m solutions of Eq. (7) over one period T for a set of linearly independent initial conditions having the following form

$$\mathbf{\Phi}(t_0,t_0) = [\,\mathbf{x}_1(t_0) \quad \mathbf{x}_2(t_0) \quad \ldots \quad \mathbf{x}_{2m}(t_0)\,] = \mathbf{I} \tag{10}$$

where $\mathbf{I}$ is the identity matrix. The eigenvalues $\boldsymbol{\lambda}$ of the monodromy matrix

$$\boldsymbol{\lambda} = \mathrm{eig}[\mathbf{\Phi}(T,0)] \tag{11}$$

are called the *Floquet's multipliers* and they determine the stability of the system. The system is asymptotically stable if and only if the magnitude of all its Floquet's multipliers is less than one, i.e. if $\max[|\boldsymbol{\lambda}|] < 1$.

The monodromy matrix can be calculated using the *precise Hsu's method* [10]. For this purpose, the period T is divided into K intervals denoted by t_k, $0 < t_0 < t_1 < \cdots < t_k = T$, where the size of the kth interval is $\Delta_k = t_k - t_{k-1}$, and K is has been assumed as $K = 50$. The monodromy matrix is obtained as [10]

$$\mathbf{\Phi}(T,0) = \prod_{k=1}^{K} \mathbf{\Phi}_k = \mathbf{I} + \mathbf{S}_{a,K} \tag{12}$$

where matrices $\mathbf{\Phi}_k$ are evaluated as

$$\mathbf{\Phi}_k = \left[\exp\left(\mathbf{A}_k \frac{\Delta_k}{n}\right)\right]^p = \mathbf{I} + \mathbf{T}_{a,k,(N+1)} \tag{13}$$

where $p = 2^N$ and N is usually assumed as $N = 20$ [10]. Matrix $\mathbf{T}_{a,k,(N+1)}$ is calculated recursively as

$$\mathbf{T}_{a,k,(N+1)} = 2\mathbf{T}_{a,k,N} + \mathbf{T}_{a,k,N}\mathbf{T}_{a,k,N} \tag{14}$$

starting with

$$\mathbf{T}_{a,k,1} = \sum_{j=1}^{N_j} \frac{(\mathbf{A}_k \Delta_k / n)^j}{j!} \tag{15}$$

where N_j is usually assumed as $N_j = 4$ [10].

Matrices $\mathbf{S}_{a,K}$ in Eq. (12) are calculated recursively as [10]

$$\mathbf{S}_{a,K} = \mathbf{S}_{a,K-1} + \mathbf{T}_{a,K,(N+1)} + \mathbf{S}_{a,K-1}\mathbf{T}_{a,K,(N+1)} \tag{16}$$

starting with

$$\mathbf{S}_{a,1} = \mathbf{T}_{a,1,(N+1)} + \mathbf{T}_{a,2,(N+1)} + \mathbf{T}_{a,1,(N+1)}\mathbf{T}_{a,2,(N+1)} \tag{17}$$

4 Experimental Verification

The RFE model of the rotor has been verified by comparing the frequency response functions of the uncracked, free-free rotor with no supporting bearings (Fig. 2) obtained experimentally (continuous line) and from the RFE model (dashed line). During the experiment the rotor suspended on a light thin string was striked with the impact hammer near the center of the 21st RFE and its vibrations were measured at the center of the 15th RFE.

Calculations were conducted for the rotor made of steel with Young's modulus $E = 2.08 \times 10^{11}$ Pa, Poisson ratio $\nu = 0.3$, and density $\rho = 7850$ kg/m^3 supported by ball bearings of radial stiffness $k_B = 3.4 \times 10^7$ N/m, and damping $d_B = 10$ Ns/m. Coefficients for the proportional damping matrix $\mathbf{D}_d$ were assumed, as $\alpha_d = 0$ 1/s and $\beta_d = 10^{-6}$ s.

Very good agreement between the experimental and numerical data is observed. The values of the first two natural frequencies agree very well (100.8 and 100 Hz for the first natural frequency, and 209.8 and 209 Hz for the second natural frequency). Due to additional stiffness, natural frequencies of the uncracked rotor supported by ball bearings are as follows: $\Omega_1 = 36$ Hz, $\Omega_2 = 135$ Hz, $\Omega_3 = 404$ Hz, $\Omega_4 = 748$ Hz, and $\Omega_5 = 882$ Hz.

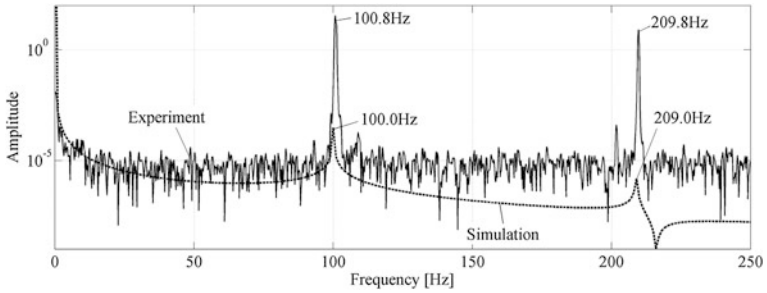

Fig. 2 Frequency transfer function of the free-free rotor (*continuous line*) and its RFE model (*dashed line*)

5 Results of the Numerical Stability Analysis

Stability analysis was performed as a function of various crack depths, from $\mu = 1$ % to $\mu = 90$ %, and parametric excitation frequency from $\eta = 1$ Hz to $\eta = 400$ Hz. A stability surface obtained numerically is presented in Fig. 3, and its two slices for the selected crack depths ($\mu = 10$ % and $\mu = 65$ %) in Fig. 4. As predicted by Eq. (1), the main areas of instability ($\max[|\Lambda|] \geq 1$) are located near principal and combination parametric resonances (Fig. 4b): at $\eta_n = |\Omega_1 + \Omega_1|/1 = 72\,\text{Hz}$, at $\eta_n = |\Omega_1 + \Omega_1|/2 = 36\,\text{Hz}$, at $\eta_n = |\Omega_3 + \Omega_4|/8 \approx 144\,\text{Hz}$, and at $\eta_n = |\Omega_3 + \Omega_5|/6 \approx 216\,\text{Hz}$. Anti-resonant combination frequencies ($\max[|\Lambda|] < 1$) are located: at $\eta_n = |\Omega_3 - \Omega_1|/1 = 368\,\text{Hz}$ and at $\eta_n = |\Omega_3 - \Omega_1|/2 = 184\,\text{Hz}$. These results confirm the previous observations outlined in the *Introduction*. Note, that for the increasing crack depth the new areas of stability/instability appear and extend as shown in Fig. 3.

The smaller values of the stability parameter $\max[|\Lambda|]$ at anti-resonant frequencies in Figs. 3 and 4 indicate the enhanced stability of the system. By

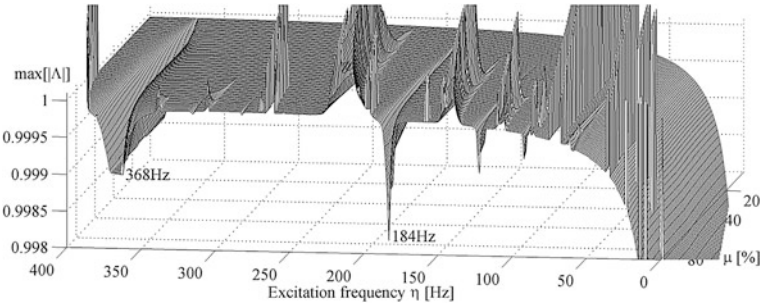

Fig. 3 Stability parameter $\max[|\lambda|]$ as the function of the parametric excitation frequency η and crack depth μ

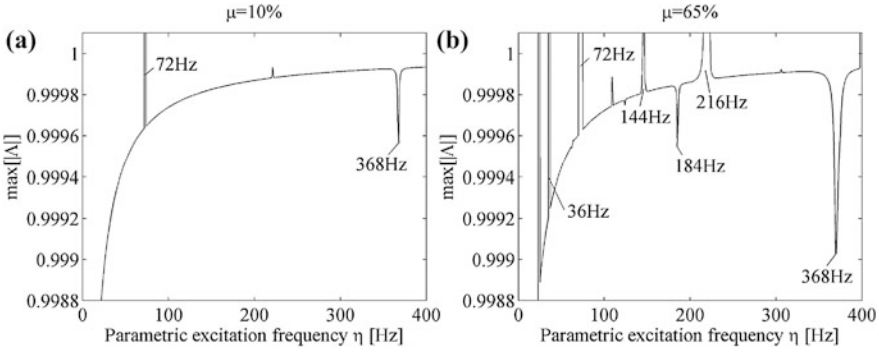

Fig. 4 Stability parameter $\max[|\lambda|]$ as the function of the parametric excitation frequency η

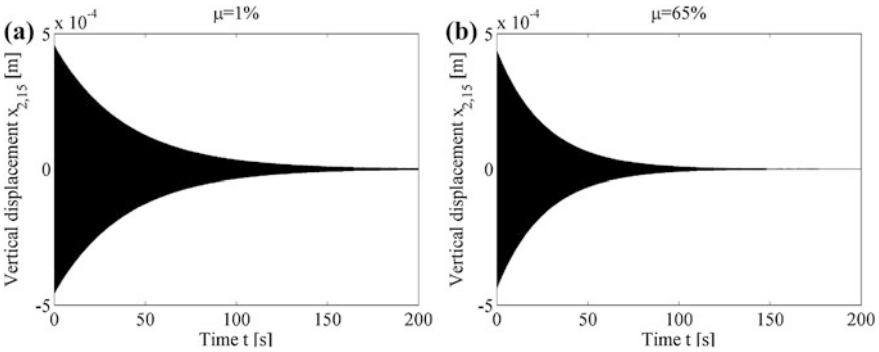

Fig. 5 Time series of the vibration signal $x_{15,2}$ at the center of the 15th RFE after an initial disturbance: **a** 1 % deep crack, **b** 65 % deep crack

parametric excitation near these frequencies the increase in damping can be observed. This effect is shown in Fig. 5 where the vertical vibration of the rotor at the middle of the 15th RFE is presented. The stiffness of the rotor is varied harmonically by $\mathbf{K}_c$ with the frequency of $\eta_n = 368$ Hz according to Eq. (1). The rotor vibrates after an initial deflection resulting from the constant vertical force of 200 N applied at $t = 0$ at the 15th RFE. For shallow cracks $\mathbf{K}_c$ is almost zero, meaning that the influence of the parametric excitation is low. In this case, the vibrations decay very slowly (Fig. 5a) due to rather a low damping in the system. However, for deeper cracks $\mathbf{K}_c$ is different than zero, resulting in an increased influence of the parametric excitation. In this case the vibrations decay faster (Fig. 5b), though the increase in the decay rate is rather low. To compare the results quantitatively, the logarithmic decrement δ, defined as

$$\delta = \frac{1}{m} \ln \left(\frac{x_{2,15,(1)}}{x_{2,15,(m)}} \right) \tag{18}$$

has been evaluated for m peaks of the rotor response, where $x_{2,15,(1)}$ and $x_{2,15,(m)}$ denote the 1st and the mth peak amplitude of the vertical displacement of the 15th RFE. For the shallow crack $\delta = 7.07 \times 10^{-4}$, while for the deeper crack $\delta = 10.61 \times 10^{-4}$.

For the excitation frequency of $\eta_n = 184$ Hz similar results are obtained, confirming an increase in damping of the cracked rotor excited parametrically.

During the simulations it was observed that gyroscopic effects disturb the presented above results. Anti-resonant frequencies are shifted from their locations calculated according to Eq. (1) and a very small increase in damping by parametric excitation is observed. Similar effects are present if the increase in the system damping matrix $\mathbf{D}_d$ is introduced (by increasing the parameter β_d). In this case the effect of damping by parametric excitation reduces, as explained by Dohnal [2].

6 Conclusions

In this numerical study the effect of the increase in damping of the rotor system with a cracked shaft excited parametrically has been demonstrated. Parametric excitation has been introduced by harmonic stiffness changes at the location of the crack, simulating the breathing behavior of the crack. Numerical analysis has been conducted with the precise Hsu's modification of the Floquet's method. Gyroscopic effects have been neglected, as they disturb the obtained results.

It has been shown that the effect of the increased damping occurs only in the presence of the crack with the properly selected parametric frequency, and if the initial overall damping in the system is low. This parametric frequency can be calculated as a difference-type combination frequency from the simple formula obtained in other papers. The increase in damping is not large, yet it clearly indicates the presence of crack.

The practical implementation of the presented method would involve the design of a device that would introduce parametric excitation to the non-rotating rotor's shaft and measure the decay rate of its vibration response up to initial deflection of the shaft.

References

1. Al-Shudeifat MA, Butcher EA (2011) New breathing functions for the transverse breathing crack of the cracked rotor system: approach for critical and subcritical harmonic analysis. J Sound Vib 330:526–544
2. Dohnal F (2008) Damping by parametric stiffness excitation: resonance and anti-resonance. J Vib Control 14(5):669–688
3. Dohnal F, Markert R (2011) Enhancement of external damping of a flexible rotor in active magnetic bearings by time-periodic stiffness variation. J Syst Design Dyn 5(5):856–865
4. Dohnal F (2012) Experimental studies on damping by parametric excitation using electromagnets. Proc Inst Mech Eng C J Mech Eng Sci. doi:10.1177/0954406212439515
5. Ecker H (2009) Parametric excitation in engineering systems. In: 20th international congress of mechanical engineering, COBEM, 15–20 November, Gramado, RS, Brazil
6. Ecker H (2011) Beneficial effects of parametric excitation in rotor systems. IUTAM Bookseries 1011:361–371
7. Ecker H, Pumhössel T (2011) Parametric excitation of a rotor system due to a periodic axial force. In: 7th European nonlinear dynamics conference, ENOC, July 24–29, Rome, Italy
8. Guo C, Al-Shudeifat MA, Yan J, Bergman LA, McFarland DM, Butcher EA (2013) Stability analysis for transverse breathing cracks in rotor systems. Eur J Mech A/Solids 42:27–34
9. Han Q, Chu F (2012) Parametric instability of a rotor-bearing system with two breathing transverse cracks. Eur. J. Mech. A/Solids 36:180–190
10. Huang JL, Su RKL, Chen SH (2009) Precise Hsu's method for analyzing the stability of periodic solutions of multi-degrees-of-freedom systems with cubic nonlinearity. Comput Struct 87:1624–1630
11. Kruszewski J, Sawiak S, Wittbrodt E (1999) Metoda sztywnych elementów skończonych w dynamice konstrukcji [The rigid finite element method in dynamics of structures]. Warsaw, WNT

12. Kulesza Z, Sawicki JT (2012) Rigid finite element model of a cracked rotor. J Sound Vib 331:4145–4169
13. Kulesza Z, Sawicki JT (2013) New finite element modeling approach of a propagating shaft crack. ASME J Appl Mech 80:021025
14. Ricci R, Pennacchi P (2012) Discussion of the dynamic stability of a multi-degree-of-freedom rotor system affected by a transverse crack. Mech Mach Theory 58:82–100
15. Sawicki JT, Friswell MI, Kulesza Z, Wroblewski A, Lekki JD (2011) Detecting cracked rotors using auxiliary harmonic excitation. J Sound Vib 330:1365–1381
16. Sawicki JT (2013) Control driven advances in smart rotating machinery. Sol. St. Phen. 198:457–467
17. Tondl A (1975) Quenching of self-excited vibrations: one- and two-frequency vibrations. J Sound Vib 42(2):261–271